Earth Planet. Sci. Lett. 676 (2026) 119787

Contents lists available at ScienceDirect

Earth and Planetary Science Letters

journal homepage: www.elsevier.com/locate/epsl

In-situ U-Pb dating of early marine carbonate cements constrains the age of the late Ediacaran lower Nama Group, Namibia

Mariana A. Yilales [a,*], Nick MW Roberts [b], Collen-Issia Uahengo [c], Nathan Rochelle-Bates [d], Fred Bowyer [e], Rachel Wood [a]

[a] School of Geosciences, University of Edinburgh, James Hutton Road, Edinburgh, EH9 3FE, UK
[b] Geochronology and Tracers Facility, British Geological Survey, Nottingham, NG125GG, UK
[c] Dept. of Geosciences, University of Namibia, Keetmanshoop, Namibia
[d] School of Earth and Environmental Sciences, University of St. Andrews St. Andrews, KY16 YTS, UK
[e] School of Earth and Environment, University of Leeds, Leeds, LS2 9JT, UK

ARTICLE INFO

Editor: Dr H Bao

Keywords:
Ediacaran
U-Pb geochronology
Carbonate cements
Nama group
Biomineralization

ABSTRACT

The middle-late Ediacaran (~580 to >533 Ma) saw the emergence and early diversification of animals (metazoans), but the tempo of this event is obscured by a paucity of datable ash beds and uncertainties in global stratigraphic correlation through specific intervals. The Nama Group, Namibia, is of fundamental importance as this succession preserves a diverse terminal Ediacaran fossil assemblage that includes the first appearance of metazoan biomineralization, a key evolutionary innovation. The precise age of the lowermost Nama Group is unknown, however, with best estimates based on global chemostratigraphic correlation and inferred depositional rates suggesting that the onset of deposition was between ca. 555 and 551 Ma. Here we use uranium-lead (U-Pb) radioisotopic dating by laser ablation inductively coupled plasma mass spectrometry (LA-ICP-MS), to date early marine pseudomorphed calcite cements from the lower Nama Group. The analyses yield an absolute age of 549.3 ± 9.8 Ma and constitute the first independent time constraint for the lowermost Nama Group. The result is consistent with current chemostratigraphic age models and validates the use of *in-situ* U-Pb dating of early marine carbonate cements to constrain depositional ages.

1. Introduction

One of the biggest challenges in understanding the Ediacaran to Cambrian rise of animals is establishing a temporal and stratigraphic framework that allows for reliable global inter-regional correlation and the accurate timing of fossil occurrences. The scarcity of datable ash beds, uncertain biostratigraphic utility of key fossils and patchiness of chemostratigraphic data across terminal Ediacaran geological sections worldwide results in considerable uncertainty (Fig. 1, e.g., Bowyer et al., 2024). The onset of metazoan biomineralisation, for example, is marked by the first occurrence of the calcified tubular fossil *Cloudina* in the Mara, informal 'Pockenbank', and lower Kliphoek members in the southwestern-most region of the Nama Group, Namibia (Figs. 1A, and 2; Germs, 1972; Kaufman et al., 2019; Bowyer et al., 2023). This interval is interpreted to have been deposited around 550 Ma, based on available global chemostratigraphic correlation to sections that host carbonate carbon isotope data calibrated in time by high-precision radioisotopic ages (e.g., Yang et al., 2021; Bowyer et al., 2023). Additional independent age constraints for the lowermost Nama Group are therefore essential for efforts that aim to understand the evolutionary timeline of metazoan biomineralization and its ecological implications.

Carbonate minerals ($CaCO_3$), like calcite, can incorporate uranium into their crystal structure upon precipitation, making them suitable for uranium-lead (U-Pb) geochronology. However, geological samples can contain multiple carbonate mineral phases with different compositions and ages, rendering bulk U-Pb methods unsuitable. For example, reef carbonate cements from the Zaris Formation of Farm Driedoornvlakte (Fig. 2B) show a paragenetic sequence of six successive cement generations from synsedimentary to early marine cement and final burial, inferred to be of variable original mineralogies (dolomite, aragonite, and calcite) and to have precipitated under dynamic redox conditions based on redox sensitive element concentrations, petrography and cathodoluminescence (CL) characteristics (Wood et al., 2018).

In combination with CL microscopy, laser ablation inductively

* Corresponding author.
E-mail address: m.a.yilales-agelvis@sms.ed.ac.uk (M.A. Yilales).

https://doi.org/10.1016/j.epsl.2025.119787
Received 13 August 2025; Received in revised form 28 November 2025; Accepted 11 December 2025
Available online 18 December 2025

coupled plasma mass spectrometry (LA-ICP-MS) can be used to date individual carbonate phases in petrographically complex samples with useful precision (~3 %–10 %; Roberts et al., 2020). Age determination requires mineral phases that have incorporated uranium with an absence or relatively low concentration of initial, or "common", lead during precipitation. This is often expressed by the ratio of parent uranium to non-radiogenic lead ($^{238}U/^{204}Pb$), otherwise denoted as μ. Ideally, the isotope system should then remain closed, with no alteration due to later diagenetic processes (Roberts et al., 2020 and references therein). The initial Pb composition and age are determined by the upper and lower intercept, respectively, of the regression isochron with the concordia curve on a Tera–Wasserburg plot (Ludwig, 1998; Roberts et al., 2020). In phases that contain common lead, robust age determinations generally require a high μ and a large spread in the initial μ

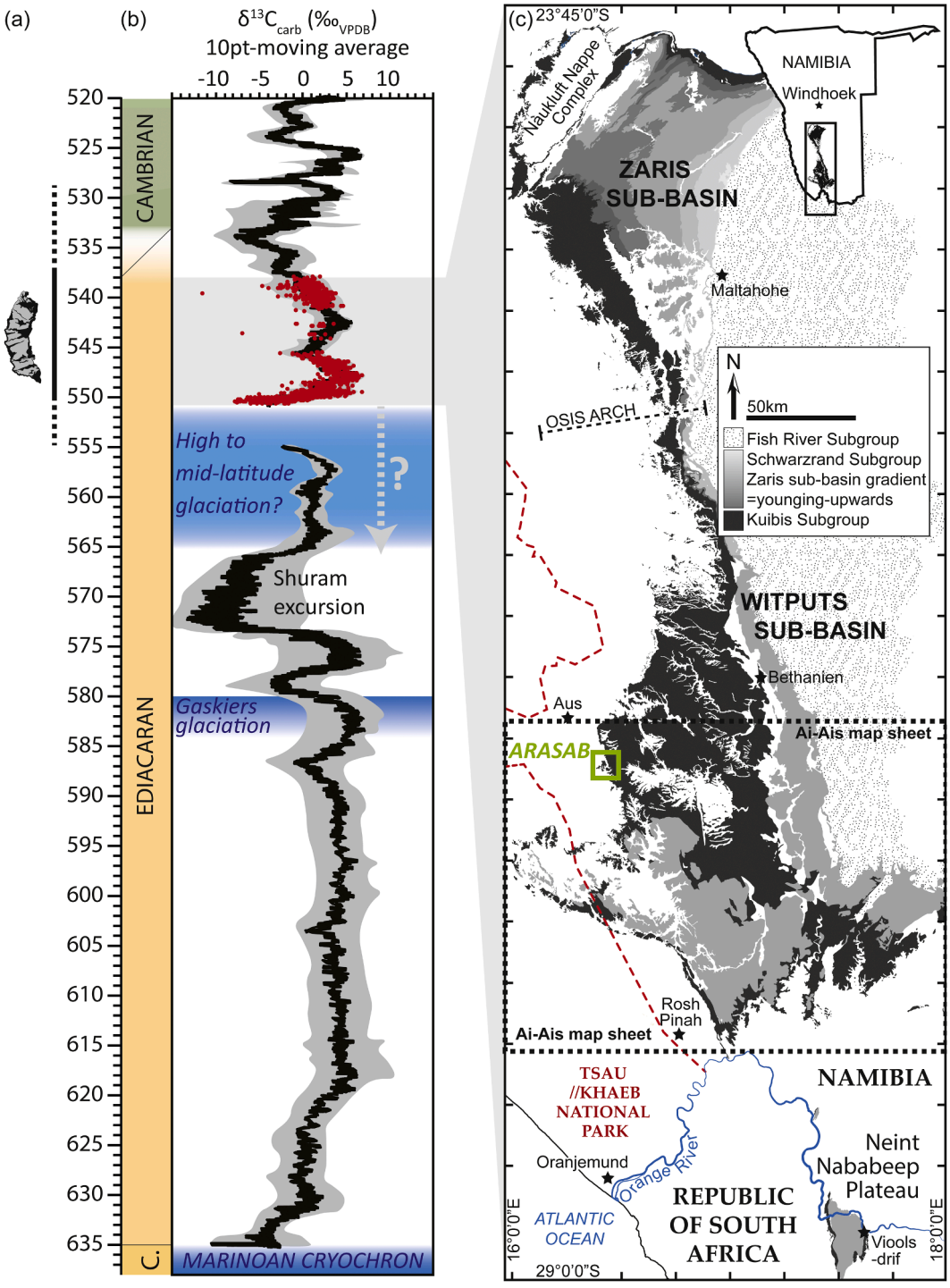

Fig. 1. Ediacaran timeline with *Cloudina*, global carbon isotope record and geological map of the Nama Group of southern Namibia and northwestern Republic of South Africa. (A) Temporal range (vertical bar) and uncertainty (dashed extensions) of the metazoan skeletal taxon, *Cloudina*. (B) Ten-point moving average (black line) and full data range (grey envelope) of global composite carbonate carbon isotope database for the Ediacaran to lower Cambrian after Bowyer et al. (2024, 2025), with Nama Group data shown in red. Uncertainty on the maximum age for the base of the Nama Group is shown as a dotted grey arrow and question mark. (C) Geological map of the Nama Group, Namibia marking the location of Farm Arasab (modified after Bowyer et al., 2023). Inset map shows the areal extent of the Nama Group in southern Namibia.

values, as these give a large spread in U/Pb ratios to define a regression, thereby providing a precise estimate of both the age and the initial lead isotopic composition. Identifying carbonate crystals that precipitated early and may preserve original elemental concentrations with limited diagenetic recrystallization (and thus limited open-system U mobility), is a crucial step in selecting appropriate targets for U-Pb dating.

Here, we used in-situ carbonate U-Pb dating to target neomorphosed early marine carbonate cements from the lowermost Nama Group of southern Namibia. The results constitute the first direct age constraint from this interval, which hosts the earliest known occurrence of metazoan biomineralization in the geological record.

2. Geological setting

The Nama Group (≥550.5 to <538 Ma; Figs. 1C and 2A) is a stratigraphic succession composed of shallow marine mixed carbonate and siliciclastic rocks deposited in a foreland basin that formed on the Kalahari Craton in the late Ediacaran and early Cambrian (Germs, 1983; Germs and Gresse, 1991). Deposition occurred within supratidal to outer ramp settings across at least two sub-basins, the Zaris in the north, and the Witputs in the south, separated by a palaeobathymetric high, the Osis Arch (Fig. 1C; Germs, 1983; Germs and Gresse, 1991). Increasing palaeodepth corresponded with increasing distance from the Osis Arch and from the centre of the Kalahari Craton to the present east. Consequently, the earliest marine deposits, which formed during diachronous transgression across the basement, are recorded in the most distal settings, including sedimentary rocks that were deposited in the southwestern Witputs sub-basin, bordering the Tsau //Khaeb National Park (Figs. 1C and 2B, Germs, 1983; Germs and Gresse, 1991; Gresse and Germs, 1993).

In the Witputs sub-basin, the lowermost Nama Group deposits comprise the Dabis and Zaris Formations, which together document two incomplete third-order sequences represented by the Kanies and Mara Members, overlain by the Kliphoek, Aar and Mooifontein Members (Fig. 1c; Saylor et al., 1995; Hall et al., 2013). *Cloudina* has been found in the Mara, 'Pockenbank', and lower Kliphoek Members (Germs, 1972; Kaufman et al., 2019).

The age of the base of the Nama Group remains uncertain. According to global chemostratigraphic correlation to sections that host high-precision zircon U-Pb ages, and based on the absence of *Cloudina* from extensive carbonate deposits that coincide with or immediately postdate the Shuram excursion (Fig. 1B), it is estimated to have formed between 555.18 ± 0.3 Ma and 550.1 ± 0.6 Ma (Parry et al., 2017; Yang et al., 2021; Bowyer et al., 2023). However, recognising the potential for biases in fossil preservation, it may be even older than 555 Ma (Bowyer et al., 2024). A high-precision zircon U-Pb age of 546.862 ± 0.088 Ma,

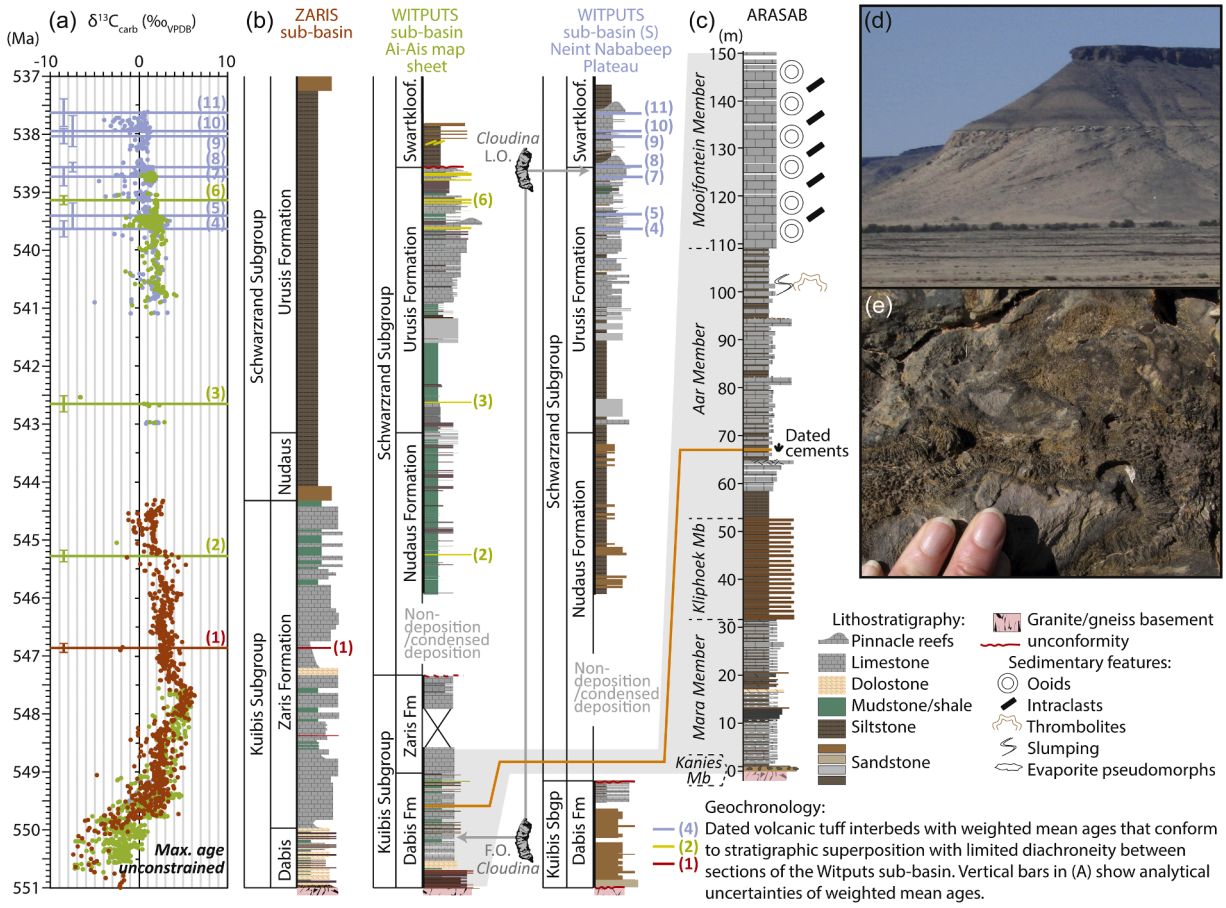

Fig. 2. Composite chemostratigraphy and sub-basin lithostratigraphy for the Ediacaran portion of the Nama Group, including expanded lithostratigraphy for the Arasab section and selected outcrop photographs. (A) Composite carbonate carbon isotope curve for the Ediacaran Nama Group from 551 to 537 Ma (updated from Bowyer et al., 2023, 2025). (B) Composite lithostratigraphic columns for each sub-basin, following section correlations depicted in the supplementary information of Bowyer et al. (2025). *Cloudina* regional first (FO) and last (LO) occurrences are pinned to the ages of horizons within individual sections of the Witputs sub-basin after Kaufman et al. (2019), Nelson et al. (2022) and Bowyer et al. (2023), depicted in full in the SI of Bowyer et al. (2025). (C) Arasab lithostratigraphy and sedimentology, showing the horizon from which carbonate cement samples were taken (modified from Bowyer et al., 2025, after original section data of Wood et al., 2015). (D) Field photograph of the nonconformity that separates basement granite from sedimentary rocks of the lower Nama Group. (E) Field photograph of early marine cements of the Aar Member at Arasab. References for ash bed zircon U-Pb CA-ID-TIMS ages are as follows: (1), (6): Bowyer et al. (2025); (2)–(10): Nelson et al. (2022); (11): Nelson et al. (in press.).

from an ash bed in the lower Hoogland Member (Zaris Formation) of the Zaris sub-basin (Fig. 2B), provides a minimum age constraint on the base of the Nama Group (Bowyer et al., 2025).

3. Materials and methods

We used in-situ U-Pb geochronology to target early marine carbonate cements, which we infer have precipitated directly from seawater, to help constrain the age of the lowermost Nama Group (see Supplementary Materials). The lowest occurrence of these cements is within the Aar Member at the Arasab section (Figs. 1C and 2B-E), which was deposited in a shallow inner-mid ramp setting in the Witputs sub-basin. The samples collected here contain first generation thick isopachous early marine calcite cements (Fig. 2E). These widespread acicular calcite cements fill both primary porosity and early fractures that formed perpendicular to bedding. The cements are brown to black in outcrop and the long axes of individual crystals measure 3.5 to 5.5 mm (Fig. 2E).

3.1. CL imaging

We examined three highly polished thin sections (75 × 50 mm; identified as Arasab 1, 2 and 3) of 140 μm thickness under a Cathodoluminescence Cold Cathode CITL 8200 MK3A mounted on a Nikon optiphot microscope. This allowed us to distinguish different carbonate mineral phases and to identify any primary compositional zonation present within cements.

3.2. In situ LA-ICP-MS U-Pb geochronology

In situ LA-ICP-MS U-Pb geochronology was conducted on the polished thin sections characterised by CL imaging following the method of Roberts et al. (2017). All dates quoted in the text are lower concordia intercept dates from Tera-Wasserburg plots, at 2 s with propagated uncertainties included. In total, we analysed 338 ablation spots by LA-ICP-MS across the different CL zonations (Table S1). Plots show Model 1 age calculations and have uncertainties quoted as age $\pm x \mid y$, where x is without systematic uncertainties and y includes the propagated systematic uncertainties. All regressions are unanchored as the spread in data permits assessment of the upper intercept accurately, and the goodness of fit of the model was evaluated with the mean square of weighted deviates (MSWD). Clear outliers (n=≤3) in Tera-Wasserburg plots were rejected from the age regressions, and are likely a consequence of analysing inclusions of a different phase. See the Supplemental Material for full data sets and detailed methodology.

4. Results

4.1. CL imaging and targeted sites

Samples contain several cement generations with distinct cathodoluminescent characteristics, which indicates that manganese (Mn) and iron (Fe) were incorporated into the carbonate crystal structures in different proportions. The paragenetic sequence is summarised in Fig. 3, and examples are shown in Fig. 4. The bright red luminescent sediment is an undifferentiated micrite with silt-grade quartz that grades to a coarser grained recrystallised calcite. Non-luminescent acicular fibrous calcite crystals nucleate from the sediment and grow into pore-space, showing bladed terminations (Fig. 4A–D). The non-luminescent acicular fibrous crystals are followed by a series of bright red-orange and non-luminescent zoned overgrowths (Fig. 3B, Fig. 4A and Fig. S1B). The final pore-occluding cement is dull-luminescent blocky calcite (Fig. 3C, Fig. S1B-C, Fig. S2A, Fig. S2B), which is followed by fine, cross-cutting veins with a bright luminescent cement fill (Fig. 3D, Fig. 4D, Fig. S1C).

We focused on the non-luminescent calcite crystals for U-Pb age determination, as they correspond to the earliest cement phase in the paragenetic sequence. Four areas across two of the thin sections were targeted (Arasab 2 and 3, Fig. S1B–C). The first region (Fig. 4A; Fig. S1B; from here on termed 'zone A') was composed of non-luminescent and well-defined crystals with hexagonal cross-sections, surrounded by a red bright luminescent overgrowth. The second region (Fig. 4B; Fig. S1C; now 'zone B') comprised poorly defined dull luminescent crystals with a more granular appearance, rich in inclusions and crossed by thin bright veins, growing into a space filled by bright red sediment. The third region (Fig. 4C; Fig. S1C; 'zone C') had large non-luminescent crystals with round terminations and poorly defined edges surrounded by highly luminescent patchy sediment. The fourth region (Fig. 4D; Fig. S1C; 'zone D') was composed of non-luminescent thin acicular crystals with rounded terminations, which were surrounded by a heterogeneously coloured bright luminescent sediment. The bright red luminescent, space-infilling sediment in zones B, C and D could have resulted from dolomitization, although we have not identified any other petrographic evidence for dolomite mineralogy.

4.2. U-Pb values of the targeted phases

The majority of the targeted phases showed low ratios of $^{207}Pb/^{206}Pb$ (Fig. 4a–d), with only 17 spots (of 209) >0.4 (Fig. 4e). We identified 5 statistical outliers across all targeted phases which were excluded from the age regression analysis. Analyses of zone A yielded a date of 549.7 ± 10.3 Ma and a MSWD of 1.7. Zone B yielded a date of 543.2 ± 15 Ma with a MSWD of 2.3. Non luminescent crystals of Zone C yielded a date of 559.1 ± 14.1 Ma with a MSWD of 2.4, while the surrounding bright

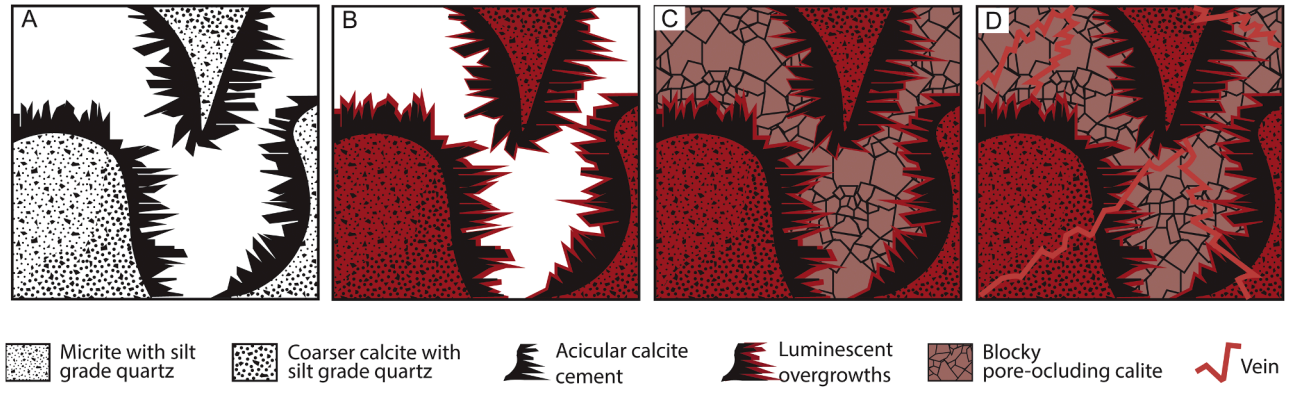

Fig. 3. Paragenetic sequence of carbonate cements in the upper Kliphoek (Aar) Member, Nama Group, at Arasab, Namibia. (A) Micrite to coarser grade calcite with silt-grade quartz and acicular fibrous calcite cements. (B) Bright luminescent red-orange overgrowths. (C) Pore-occluding blocky calcite cement. (D) Bright luminescent veins. Colours in (B)–(D) follow CL characteristics.

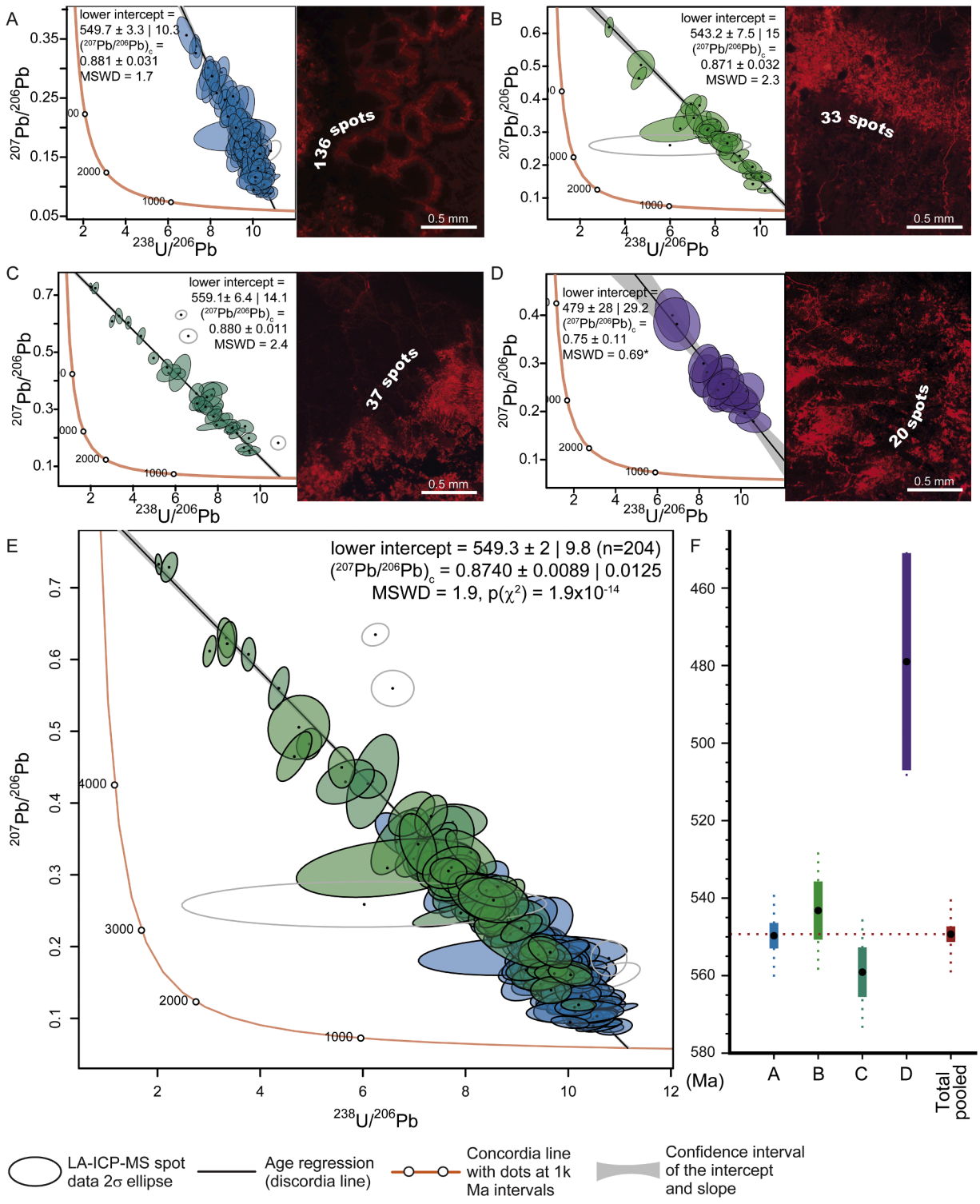

Fig. 4. CL photomicrographs of targeted carbonate cements from Farm Arasab and Tera-Wasserburg plots. (A)–(D) Tera-Wasserburg plots with corresponding isochron line and lower intercept dates (2σ) along cathodoluminescence (CL) photomicrographs and the distribution of sample spots within four targeted areas of non to dull luminescent calcite crystals analysed by laser ablation. (E) Tera-Wasserburg plot and lower intercept date combining all 204 pooled laser ablation spots from Zones A, B and C. The spots and ellipses in Tera-Wasserburg space are colour coded according to target crystals in panels (A) to (C). Empty ellipses represent statistical outliers that are not included in the calculation of dates. The p-value of chi-squared (χ^2) for the isochron fit was < 0.05 unless indicated by an '*' beside the MSWD value (D). Tera-Wasserburg plots were constructed in IsoplotR (Ludwig, 1998; Vermeesch, 2018). (F) Schematic summarizing the chronology of cement generations by showing the age determinations of measured crystal populations, with colour code for each zone consistent with panels (A) to (E). Solid lines represent the analytical uncertainty and dotted lines the propagated uncertainty.

sediment (not shown, but see supplementary data) yielded a date of 549 ± 14 Ma and a MSWD of 1.8. Zone D needle-like crystals yielded a date of 479 ± 29.2 Ma and a MSWD of 0.69. The pooled older carbonate population, zones A to C, give a date of 549.3 ± 9.8 Ma with a MSWD of 1.9. All the other analysed carbonate phases were unsuccessful in yielding meaningful dates with uncertainties being larger than the entire known depositional duration of the Nama Group (Fig. S3).

5. Discussion

Petrographic features, including crystal growth directly from primary sediment and lack of luminescence, indicate that the first cement phase is an early marine aragonite cement that has been pseudomorphosed. The U-Pb data gathered from these cements yield high-precision (in terms of carbonate U-Pb) late Ediacaran ages, as shown by the relatively small level of uncertainty (analytical uncertainties <2 %, 2σ) of our analyses. The pooled date of the oldest cements, 549.3 ± 9.8 Ma, is consistent with current age frameworks based on global chemostratigraphic correlation (Fig. 1B). Limited scatter in the data (as shown by MSWDs of ~ 2) indicates that if any resetting of the U-Pb system occurred during neomorphism, it must have taken place very shortly after precipitation and/or was pervasive. This supports petrographic evidence and the reconstructed paragenetic sequence, which shows that we have targeted the oldest cement crystal phase precipitated from seawater (See supplementary information for U-Pb dates of additional phases).

The variable U/Pb ratios and moderate to high proportions of radiogenic lead in the successful samples aided in constraining robust regressions and lower intercept dates. Initial lead isotope compositions, as determined by the upper intercept in Tera-Wasserburg space, have values (pooled data has $^{207}Pb/^{206}Pb = 0.873$) that are similar to the modelled average terrestrial Pb composition (Stacey and Kramers, 1975). The lack of markedly radiogenic Pb supports our interpretation of limited open-system remobilisation or contamination of extraneous Pb.

High Th/U values from some samples (see supplementary material) could suggest that we ablated a significant proportion of detrital material. This detrital material may be contributing variable compositions of common Pb to our measurements, potentially leading to overdispersion of the data. However, the fairly low MSWDs (~2), high proportion of radiogenic Pb and typical terrestrial initial Pb compositions suggest that the detrital component has not impacted the age determinations significantly.

Zone A and C calcite cements provided the oldest dates and are within uncertainty of each other. The larger range of dates for zone C cements is partly due to lower proportions of radiogenic lead. When considering the fully propagated uncertainties, Zone B overlaps with the older date, but the intercept indicates a younger date. We attribute this difference to the presence of inclusions of a different phase and veins that are visible under CL. The inclusions and veins formed during a later diagenetic event, possibly in response to active foreland tectonics that characterised ongoing Nama Basin subsidence. The surrounding bright luminescent sediments in zones B, C, and D have likely undergone dolomitization (although we could not identify any other petrographic evidence for dolomite mineralogy), and yielded a date of 549 ± 14 Ma (Fig. S2a). It is possible that small inclusions (5–20 μm) of the younger dolomitized sediment skewed the isotopic composition of the older cements during laser ablation. The marine redox-chemical landscape of the Nama Basin during deposition of the Kuibis Subgroup was heterogeneous, with shallower water masses being subjected to anoxic incursions that may have been responsible for intervals of widespread early dolomitization (Wood et al., 2018). A diagenetic event associated with early dolomitization might explain the seemingly younger date of the bright luminescent sediment, which has age ranges that overlap with the oldest calcite cement. The calculated date after excluding zone B from the pooled acicular cement population is 549.9 ± 9.8 Ma (see the Summary Table in Supplementary Materials and Fig. S3). Thus, excluding the zone B spot analyses from the pooled data does not have an impact on the calculated date and associated uncertainty for the acicular cements. The spots from zone D yield a much younger date and the U-Pb isotopic compositions could reflect a later diagenetic event.

6. Conclusions

Constraining the age of the lowermost Nama Group is crucial to understanding the timing and evolutionary rates of the Ediacaran-Cambrian faunal transition. We present the first independent age constraint for the lowermost Nama Group (southern Namibia), which is known to contain the earliest occurrence of biomineralization in the geological record. Early marine fibrous calcite cements yield an *in-situ* carbonate U-Pb date of 549.3 ± 9.8 Ma for the Aar Member of the Dabis Formation, validating previous indirect age estimations, which were based on global chemostratigraphic correlation, and supporting proposed inter-basin stratigraphic alignments (Bowyer et al., 2025). Some carbonate cements within the samples may reflect later diagenetic processes, potentially involving basin-wide redox and/or tectonic changes. However, we interpret the robust U-Pb dates from the older fibrous calcites to reflect early and pervasive neomorphism of aragonite, followed by essentially closed system behaviour of the U-Pb system. Consequently, this date represents the age of a diagenetic phase of early cement growth, and it therefore approximates the depositional age of the lower Aar Member. Thus, our results provide the first independent age constraint for the deposition of the lower Nama Group and showcase the utility of early marine carbonate cements for constraining depositional ages via *in-situ* U-Pb geochronology.

CRediT authorship contribution statement

Mariana A. Yilales: Writing – original draft, Visualization, Investigation, Formal analysis, Conceptualization. **Nick MW Roberts:** Writing – review & editing, Validation, Methodology, Investigation. **Collen-Issia Uahengo:** Writing – review & editing, Resources. **Nathan Rochelle-Bates:** Writing – review & editing, Validation. **Fred Bowyer:** Writing – review & editing, Visualization. **Rachel Wood:** Writing – review & editing, Supervision, Resources.

Declaration of competing interest

The authors declare that they have no known competing financial interests or personal relationships that could have appeared to influence the work reported in this paper.

Acknowledgements

MY acknowledges support from the ANID Becas Chile/Doctorado en el Extranjero 72210327, RW thanks NERC Project NE/Z000122/1 and NEIF grant IP/2377/0321, FB acknowledges support from UKRI Project EP/Y008790/1. The NEIF was funded through grant NE/Y005449/1.

Supplementary materials

Supplementary material associated with this article can be found, in the online version, at doi:10.1016/j.epsl.2025.119787.

Data availability

The data used has been attached as an excel file at the Attach File step.

References

Bowyer, F.T., Messori, F., Wood, R., Linnemann, U., Rojo-Perez, E., Zieger-Hofmann, M., Zieger, J., Ndeunyema, J., Shipanga, M., Mataboge, B., Condon, D., Rose, C.V.,

Uahengo, C.-I., Gaynor, S.P., Müller, I.A., Geyer, G., Vennemann, T., Davies, J.H.F.L., Ovtcharova, M., 2025. Foundational uncertainties in terminal Ediacaran chronostratigraphy revealed by high-precision zircon UPb geochronology of the Nama Group, Namibia. Earth. Sci. Rev., 105169 https://doi.org/10.1016/j.earscirev.2025.105169.

Bowyer, F.T., Uahengo, C.-I., Kaputuaza, K., Ndeunyema, J., Yilales, M., Alexander, R.D., Curtis, A., Wood, R.A., 2023. Constraining the onset and environmental setting of metazoan biomineralization: the Ediacaran Nama Group of the Tsaus Mountains, Namibia. Earth. Planet. Sci. Lett. 620, 118336. https://doi.org/10.1016/j.epsl.2023.118336.

Bowyer, F.T., Wood, R.A., Yilales, M., 2024. Sea level controls on Ediacaran-Cambrian animal radiations. Sci. Adv. 10 (31), eado6462. https://doi.org/10.1126/sciadv.ado6462.

Germs, G.J., 1972. New shelly fossils from Nama Group, south west Africa. Am. J. Sci. 272 (8), 752–761.

Germs, G.J.B., 1983. Implications of a sedimentary facies and depositional environmental analysis of the Nama Group in South West Africa/Namibia. Special Publications Geological Society of South Africa.

Germs, G.J.B., Gresse, P.G., 1991. The foreland basin of the Damara and Gariep orogens in Namaqualand and southern Namibia; stratigraphic correlations and basin dynamics. South African J. Geol. 94 (2–3), 159–169.

Gresse, P.G., Germs, G.J.B., 1993. The Nama Foreland Basin—Sedimentation, Major Unconformity Bounded Sequences and Multisided Active Margin Advance. Precambrian. Res. 63 (3–4), 247–272. https://doi.org/10.1016/0301-9268(93)90036-2.

Hall, M., Kaufman, A.J., Vickers-Rich, P., Ivantsov, A., Trusler, P., Linnemann, U., Hofmann, M., Elliott, D., Cui, H., Fedonkin, M., Hoffmann, K.-H., Wilson, S., Schneider, G., Smith, J., 2013. Stratigraphy, palaeontology and geochemistry of the late Neoproterozoic Aar Member, southwest Namibia: reflecting environmental controls on Ediacara fossil preservation during the terminal Proterozoic in African Gondwana. Precambrian. Res. 238, 214–232. https://doi.org/10.1016/j.precamres.2013.09.009.

Kaufman, A.J., Kriesfeld, L., Vickers-Rich, P., Narbonne, G., 2019. When life got hard: an environmental driver for metazoan biomineralization. Estudios Geológicos 75 (2). https://doi.org/10.3989/egeol.43597.556. Article 2.

Ludwig, K.R., 1998. On the Treatment of Concordant Uranium-Lead Ages. Geochim. Cosmochim. Acta 62 (4), 665–676. https://doi.org/10.1016/S0016-7037(98)00059-3.

Nelson, L.L., Ramezani, J., Almond, J.E., Darroch, S.A.F., Taylor, W.L., Brenner, D.C., Furey, R.P., Turner, M., Smith, E.F., 2022. Pushing the boundary: a calibrated Ediacaran-Cambrian stratigraphic record from the Nama Group in northwestern Republic of South Africa. Earth. Planet. Sci. Lett. 580, 117396. https://doi.org/10.1016/j.epsl.2022.117396.

Parry, L.A., Boggiani, P.C., Condon, D.J., Garwood, R.J., Leme, J., de, M., McIlroy, D., Brasier, M.D., Trindade, R., Campanha, G.A.C., Pacheco, M.L.A.F., Diniz, C.Q.C., Liu, A.G., 2017. Ichnological evidence for meiofaunal bilaterians from the terminal Ediacaran and earliest Cambrian of Brazil. Nat. Ecol. Evol. 1 (10), 1455–1464. https://doi.org/10.1038/s41559-017-0301-9.

Roberts, N.M.W., Drost, K., Horstwood, M.S.A., Condon, D.J., Chew, D., Drake, H., Milodowski, A.E., McLean, N.M., Smye, A.J., Walker, R.J., Haslam, R., Hodson, K., Imber, J., Beaudoin, N., Lee, J.K., 2020. Laser ablation inductively coupled plasma mass spectrometry (LA-ICP-MS) U–Pb carbonate geochronology: strategies, progress, and limitations. Geochronology 2 (1), 33–61. https://doi.org/10.5194/gchron-2-33-2020.

Roberts, N.M.W., Rasbury, E.T., Parrish, R.R., Smith, C.J., Horstwood, M.S.A., Condon, D.J., 2017. A calcite reference material for LA-ICP-MS U-Pb geochronology. Geochemistry, Geophysics, Geosystems 18 (7), 2807–2814. https://doi.org/10.1002/2016gc006784.

Saylor, B.Z., Grotzinger, J.P., Germs, G.J.B., 1995. Sequence stratigraphy and sedimentology of the Neoproterozoic Kuibis and Schwarzrand Subgroups (Nama Group), southwestern Namibia. Precambrian. Res. 73 (1), 153–171. https://doi.org/10.1016/0301-9268(94)00076-4.

Stacey, J.S., Kramers, J.D., 1975. Approximation of terrestrial lead isotope evolution by a two-stage model. Earth. Planet. Sci. Lett. 26 (2), 207–221. https://doi.org/10.1016/0012-821X(75)90088-6.

Vermeesch, P., 2018. IsoplotR: a free and open toolbox for geochronology. Geosci. Front. 9 (5), 1479–1493. https://doi.org/10.1016/j.gsf.2018.04.001.

Wood, R.A., Poulton, S.W., Prave, A.R., Hoffmann, K.H., Clarkson, M.O., Guilbaud, R., Lyne, J.W., Tostevin, R., Bowyer, F., Penny, A.M., Curtis, A., Kasemann, S.A., 2015. Dynamic redox conditions control late Ediacaran metazoan ecosystems in the Nama Group, Namibia. Precambrian. Res. 261, 252–271. https://doi.org/10.1016/j.precamres.2015.02.004.

Wood, R., Bowyer, F., Penny, A., Poulton, S.W., 2018. Did anoxia terminate Ediacaran benthic communities? Evidence from early diagenesis. Precambrian. Res. 313, 134–147. https://doi.org/10.1016/j.precamres.2018.05.011.

Yang, C., Rooney, A.D., Condon, D.J., Li, X.-H., Grazhdankin, D.V., Bowyer, F.T., Hu, C., Macdonald, F.A., Zhu, M., 2021. The tempo of Ediacaran evolution. Sci. Adv. 7 (45), eabi9643. https://doi.org/10.1126/sciadv.abi9643.